RESEARCH ARTICLE

Voltage-clamp recordings of light responses from wild-type and mutant mouse cone photoreceptors

Norianne T. Ingram[1,2], Alapakkam P. Sampath[2], and Gordon L. Fain[1,2]

We describe the first extensive study of voltage-clamp current responses of cone photoreceptors in unlabeled, dark-adapted mouse retina using only the position and appearance of cone somata as a guide. Identification was confirmed from morphology after dye filling. Photocurrents recorded from wild-type mouse cones were biphasic with a fast cone component and a slower rod component. The rod component could be eliminated with dim background light and was not present in mouse lines lacking the rod transducin-α subunit ($Gnat1^{-/-}$) or connexin 36 ($Cx36^{-/-}$). Cones from $Gnat1^{-/-}$ or $Cx36^{-/-}$ mice had resting membrane potentials between −45 and −55 mV, peak photocurrents of 20–25 picoamps (pA) at a membrane potential V_m = −50 mV, sensitivities 60–70 times smaller than rods, and a total membrane capacitance two to four times greater than rods. The rate of activation (amplification constant) was largely independent of the brightness of the flash and was 1–2 s^{-2}, less than half that of rods. The role of Ca^{2+}-dependent transduction modulation was investigated by recording from cones in mice lacking rod transducin (Gnat1), recoverin, and/or the guanylyl-cyclase–activating proteins (GCAPs). In confirmation of previous results, responses of $Gnat1^{-/-};Gcaps^{-/-}$ cones and triple-mutant $Gnat1^{-/-};Gcaps^{-/-};Rv^{-/-}$ cones recovered more slowly both to light flashes and steps and were more sensitive than cones expressing the GCAPS. Cones from all four mouse lines showed significant recovery and escaped saturation even in bright background light. This recovery occurred too rapidly to be caused by pigment bleaching or metaII decay and appears to reflect some modulation of response inactivation in addition to those produced by recoverin and the GCAPs. Our experiments now make possible a more detailed understanding of the cellular physiology of mammalian cone photoreceptors and the role of conductances in the inner and outer segment in producing cone light responses.

Introduction

Most mammalian retinas have two kinds of photoreceptors: highly sensitive rods, which primarily function in dim light, and less-sensitive but faster-decaying cones, which respond in brighter light to more rapid changes in illumination and mediate wavelength discrimination in many species including humans. Although cones play a central role in our daytime vision, we know significantly less about their cellular physiology and mechanism of transduction. This is because in most mammalian retinas, cones represent only a small fraction of the total number of photoreceptors (mouse, 3%; see Ortín-Martínez et al., 2014). Their small number makes more difficult both physiological recording and biochemical measurements.

Although recent results from primate cones have greatly extended our understanding of normal cone function (Angueyra and Rieke, 2013; Sinha et al., 2017; Baudin et al., 2019), it would be useful to study cone photoresponses in a genetically tractable model where elements of phototransduction can be modified or deleted. The mouse retina offers these advantages, because genetic

tools are available to explore mechanisms of phototransduction and other aspects of retinal function. Much of interest has been learned about mouse cone transduction from previous measurements with suction-electrode recording (Nikonov et al., 2005, 2006), perforated-patch voltage recording (Cangiano et al., 2012; Asteriti et al., 2014), and whole-retina isolated photoreceptor recording (for example, Sakurai et al., 2011, 2015; Morshedian et al., 2019). These experiments have provided new information about the physiological significance of rod/cone coupling (Asteriti et al., 2014, 2017) and the role of transduction proteins in producing the cone light response (Sakurai et al., 2011, 2015). Recordings from whole $Gnat1^{-/-}$ retinas lacking rod responses in the presence of synaptic and Müller-cell blockers have been particularly valuable in studying mechanisms of cone pigment regeneration (Wang et al., 2009; Wang and Kefalov, 2009; Morshedian et al., 2019). All of these methods leave the voltage of the cone free to vary during the light response. Changes in voltage are important indicators of cone function, because the cone membrane potential is ultimately

[1]Department of Integrative Biology and Physiology, University of California, Los Angeles, Los Angeles, CA; [2]Department of Ophthalmology and Jules Stein Eye Institute, University of California, Los Angeles, Los Angeles, CA.

Correspondence to Gordon L. Fain: gfain@ucla.edu.

responsible for determining release of synaptic transmitter onto second-order horizontal and bipolar cells. Voltage measurements cannot however be used to provide quantitative measurements of the conductance of the channels gated by cyclic guanosine monophosphate (cGMP) in the cone outer segment or of voltage-dependent and Ca^{2+}-activated conductances in the cone inner segment.

It would therefore be useful to develop a method to record voltage-clamp currents from mouse cones. Although one demonstration of voltage-clamp recording from mouse cones has been previously published (Fig. 8 C of Asteriti et al., 2014), responses were only a few pA in magnitude. To provide a more extensive study of cone voltage-clamp currents, we have developed a new methodology relying only on intrinsic visual cues without fluorescent labeling so that we can record from single mouse cones entirely under infrared illumination to preserve dark-adapted sensitivity. Cone photoreceptors can be targeted with a 90% success rate based on the shape and position of their somata alone. We have used this method to characterize the electrical properties and light-dependent changes in conductance of cones to flashes and steps of light in WT mice and several mutant mouse lines. We show that WT mouse cones receive input from rods through gap junctions, as others have previously described (Asteriti et al., 2014), and that we could eliminate this input by recording from retinas lacking the rod transducin α subunit ($Gnat1^{-/-}$) or connexin 36 gap junctions ($Cx36^{-/-}$; Asteriti et al., 2017). We then mated the $Gnat1^{-/-}$ or $Cx36^{-/-}$ animals to other mutant lines to record the light-dependent changes in cone conductance in cells lacking one or both of the small-molecular-weight Ca^{2+}-binding proteins recoverin and the guanylyl-cyclase–activating proteins (GCAPs). We show that even in the absence of both recoverin and the GCAPs, cone voltage-clamped currents still escape saturation in bright light. Our method will allow an extensive exploration of the normal and mutant physiology of mouse cones, which will facilitate a more detailed understanding of the photoreceptors we primarily depend upon for most of our visual behavior.

Materials and methods

Animals
Experiments were performed in accordance with rules and regulations of the National Institutes of Health guidelines for research animals, as approved by the Institutional Animal Care and Use Committee of the University of California, Los Angeles (protocol 1993–230-81). Mice were kept under cyclic light (12 h on/12 h off) with ad lib food and water. WT mice (C57BL/6J) were purchased from The Jackson Laboratory (Bar Harbor, ME) and were not screened for the absence of the rd8 mutation (Chang et al., 2002). Mice in which the rod-specific α subunit of the G protein transducin had been deleted ($Gnat1^{-/-}$) were originally made in the laboratory of Janice Lem at Tufts University (Boston, MA; Calvert et al., 2000) and were obtained locally from the laboratory of Dr. Gabriel Travis at University of California, Los Angeles (Los Angeles, CA). Since these animals lack functional rod transducin, their rods (with only very rare exceptions) are completely insensitive to light (Calvert et al., 2000). Jeannie Chen of the University of Southern California (Los Angeles, CA) provided

$Gcaps^{-/-}$ mice without the GCAPs (Mendez et al., 2001) and $Rv^{-/-}$ mice without recoverin (Makino et al., 2004). These mice were bred onto the $Gnat1^{-/-}$ background to create lines that were double knockout ($Gnat1^{-/-};Rv^{-/-}$ and $Gnat1^{-/-};Gcaps^{-/-}$) or triple knockout ($Gnat1^{-/-};Rv^{-/-};Gcaps^{-/-}$). Mice lacking the gap junction protein connexin36 ($Cx36^{-/-}$) were generated by David Paul from Harvard University (Cambridge, MA; Deans et al., 2002) and obtained from Samuel Wu at Baylor University College of Medicine (Houston, TX). During the creation of double- and triple-mutant strains, at least three generations were produced before data collection commenced. Mutations received from other investigators had been bred for many generations before we received them. Genotypes were confirmed with standard PCR protocols described in the original reports of the various mutations. Once genotypes were confirmed, strains were kept as homozygous breeding pairs. It is possible that deletion of the rod $Gnat1$ gene or the gap-junctional $Cx36$ gene altered the expression of cone transduction proteins, but we have no way of testing this possibility because of the difficulty of doing biochemistry on the small number of cones in mouse. We believe, however, that the similarity of the waveforms of $Gnat1^{-/-}$ and $Cx36^{-/-}$ cones shown in Fig. 2, B and C supports our view that changes in cone transduction protein expression are likely to have been small.

Solutions
Retinal slices were cut in HEPES-buffered Ames medium, which contained 2.38 g HEPES per liter and was balanced with 0.875 g NaCl per liter to give an osmolarity of 284 ± 1 mOsm (pH 7.35 ± 0.05). Ames-HEPES was kept on ice and continuously bubbled with 100% O_2. Retinal slices were superfused at 2 ml/min in the recording chamber with Ames medium, which was continuously bubbled with 95% O_2/5% CO_2 and buffered with 1.9 g per liter sodium bicarbonate to maintain pH between 7.3 and 7.4. The internal solution for recording pipettes was a potassium aspartate solution consisting of (in mM) 125 potassium aspartate, 10 KCl, 10 HEPES, 5 NMDG-HEDTA, 0.5 $CaCl_2$, 0.5 $MgCl_2$, 0.1 ATP-Mg, 0.5 GTP-TRIS, 2.5 NADPH (pH 7.3 ± 0.02 with NMDG-OH; 280 ± 1 mOsm). In a few preliminary experiments, higher levels of nucleotides were used with no difference in responses recorded. All values of cone membrane potential V_m have been corrected for the liquid junction potential (Neher, 1992), which was measured to be approximately 10 mV for this internal solution.

Whole-cell patch clamp in retinal slices
After a period of overnight dark adaptation, male and female mice in approximately equal numbers between 1 and 4 mo old were euthanized by cervical dislocation. Eyes were marked to indicate the dorsal-ventral axis. After enucleation, the anterior portion of the eye including the lens was removed under infrared illumination, and the remaining eyecup was stored at 32°C in a custom, light-tight storage container that allowed for the gassing of solutions. For each slice preparation, half the eyecup was isolated with a #10 scalpel, and the retina was gently separated from the retinal pigmented epithelium with fine tweezers. The isolated retinal piece was embedded in 3% of low-temperature-gelling agar in Ames-HEPES. In cold Ames-HEPES,

200-µm-thick slices were cut with a vibratome (VT-1000S; Leica); the retina was cut vertically to maintain neural circuitry. Cut slices were either transferred to dishes for immediate recording or stored in the light-tight container with the remaining pieces of the eyecups. During recordings, slices were stabilized with handmade anchors, and the bath solution was maintained at 35 ± 1°C by a feedback temperature controller (TC-324B; Warner Instruments). Animals were typically sacrificed in the late morning. Several experiments performed in the late evening did not yield different response characteristics.

Electrical recording

Cones were identified in slices under infrared illumination with a 850- to 950-nm light-emitting diode (LED). No labels, markers, or tracers were needed, and standard microscopy was used without differential-interference contrast (DIC) or phase contrast (see Imaging below). Cones were typically identified from the morphology of their somata. A cone soma is slightly larger than a rod soma and is more ellipsoid in shape. Cone somata are located only in the outmost layers of the outer nuclear layer (ONL); many are found directly against the external limiting membrane (Applebury et al., 2000). The most distinguishing features, however, were the patterns seen in the somata themselves. Under our optical conditions, healthy rod somata displayed a diffuse gradation of optical density. Cone somata had instead a distinct striping pattern, which likely arises from differences in the looser chromatin packing in the nuclei of these photoreceptors (Solovei et al., 2009; Hughes et al., 2017). Our method yielded an ∼90% accurate identification rate and could be applied across various mouse retinal genotypes.

Filamented borosilicate glass capillaries (BF120-69-10; Sutter Instruments) were pulled the day of the experiment with a P-97 Flaming/Brown micropipette puller (Sutter Instruments). Pipettes used to record mouse photoreceptors generally had a resistance of 15–19 MΩ. Cones were patch clamped in the whole-cell configuration and could be recorded in voltage-clamp and current-clamp modes. During voltage clamp, cones were held at a clamp potential of –40 mV (V_m = –50 mV) unless otherwise indicated. This value spans the membrane potentials of WT animals and the various mutants, which were as follows: WT (C57BL/6J), –49.7 ± 2.3 mV, n = 22; $Gnat1^{-/-}$, –53.4 ± 4.2 mV, n = 11; and $Cx36^{-/-}$, –45.2 ± 1.5, n = 66. There were no significant differences in the means for the various animal lines (p = 0.12–0.71, ANOVA). These values are close to those previously reported for primate cones (Schneeweis and Schnapf, 1995).

The exact value of the holding potential we used could have influenced the resting outer-segment Ca^{2+} concentration because of the voltage dependence of sodium-calcium-potassium exchange (NCKX) transport (Cervetto et al., 1989), but we think that this effect is likely to be small. The experiments of Perry and McNaughton (1991) and our own model calculations in collaboration with Jürgen Reingruber indicate that NCKX currents are ∼10% of the total voltage-clamp current and make only a small contribution to the waveform of the light response. Moreover, normalized cone response waveforms within the physiological range are nearly superimposable, because unlike salamander rods (Baylor and Nunn, 1986), the light-dependent conductance of

mouse cones is not voltage dependent (Ingram et al., 2019). As a consequence, the exact value we have chosen for the holding potential has little effect on the results we have reported.

Series resistance was compensated at 75–80% and did not produce oscillations at these values. Photocurrent responses were <50 pA, and series resistance error would have been <1 mV even without compensation. Light responses from mouse cones in whole-cell configuration were generally stable for 5–10 min, with occasional cells lasting nearly 15 min. The relatively high resistance of our patch pipettes, which was sufficiently low to limit series-resistance error but probably high enough to restrict washout of nucleotides and other large-molecular-weight molecules, may explain at least in part the stability of our recordings. Experiments were terminated after loss of response amplitude or slowing of response kinetics. Data were filtered at 500 Hz (8-pole Bessel, Frequency Devices 900), sampled at 10 kHz, and recorded in an open-source, MATLAB-based program called Symphony Data Acquisition System (http://www.open-ephys.org/symphony/).

Light stimuli

Light stimuli were either brief flashes (5 ms) or several-second presentations of monochromatic light. Monochromatic light was provided by ultrabright LEDs driven with a linear feedback driver (Opto-LED; Carin Research). LEDs emitting 365-nm and 505-nm light were used to test the spectral sensitivity of individual cells and determine whether each cone expressed S, M, or a mixture of opsin types (Applebury et al., 2000). After brief spectral testing, subsequent illumination was supplied by a 405-nm-emitting LED. This wavelength is near the isosbestic point of S and M pigments in mouse and stimulates both opsin types with approximately the same efficacy.

Light intensities of individual LEDs were calibrated with a photodiode (Graseby Optronics 268R). The measured value of photons per second was then converted to pigment molecules bleached per second (P^* s^{-1}) from the cone collecting area determined in the following way. Single-photon responses of rods were recorded from the same preparations as those used for WT and $Cx36^{-/-}$ cones. By scaling the time-dependent variance to the squared mean response in rods (Mendez et al., 2000; Cao et al., 2008; Okawa et al., 2010), we estimated the rod collecting area to be 0.2 rhodopsins activated per µm² in our slices. This value is in close agreement with previous measurements made in mouse retinal slice preparations (Cao et al., 2008; Okawa et al., 2010).

Two further adjustments were then made to convert 0.2 Rh*/µm² into a cone collecting area. To account for the approximately fivefold decrease in quantum efficiency and pigment activation by 405 nm compared with the spectral maxima of the S and M cones at 355 nm and 508 nm, the collecting area was multiplied by 0.2 (Govardovskii et al., 2000). This value was further multiplied by the fraction 14/38, which is the ratio of the cone-to-rod outer-segment volume (Nikonov et al., 2006), giving a final collecting area of 0.013 P*/µm² for cones stimulated with 405-nm light in 200-µm slices. This is the value we have used in calculating the light intensities for our figures. It is however important to note that the numbers of pigment molecules actually bleached by our flashes is likely to be somewhat

Table 1. **Mouse cone flash response parameters**

Genotype	n	r_{max} (pA)	$I_{1/2}$ (P*)	Time to peak (ms)	τ_{rec} (ms)	A (s^{-2})	R_{in} (MΩ)	C_m (pF)
C57BL/6J cones	13	30 ± 2.0	470 ± 89	41 ± 1.9	200 ± 18	5.3 ± 0.4	850 ± 120	7.5 ± 0.5
				24 ± 0.6	155 ± 28			
C57BL/6J rods	5	17 ± 1.6	14 ± 2.4	200 ± 17	130 ± 23	4.6 ± 0.3	4,000 ± 680	3.6 ± 0.3
				140 ± 20	260 ± 59			
Gnat1$^{-/-}$ cones	25	21 ± 0.9	940 ± 110	59 ± 3.2	28 ± 1.9	2.1 ± 0.2	1,500 ± 350	6.9 ± 0.6
				33 ± 1.9	42 ± 1.9			
Cx36$^{-/-}$ cones	30	26 ± 1.3	990 ± 93	79 ± 4.8	64 ± 8.5	1.1 ± 0.1	850 ± 130	7.5 ± 0.3
				50 ± 1.9	61 ± 3.4			
Gnat1$^{-/-}$;Rv$^{-/-}$ cones	36	20 ± 0.9	1,100 ± 110	55 ± 4.6	33 ± 3.1	1.7 ± 0.1	770 ± 140	6.2 ± 0.3
				30 ± 2.4	47 ± 2.2			
Gnat1$^{-/-}$;Gcaps$^{-/-}$ cones	30	14 ± 0.9	740 ± 120	79 ± 5.5	125 ± 28	1.8 ± 0.1	1,200 ± 310	6.6 ± 0.4
				43 ± 2.4	98 ± 6.4			
Gnat1$^{-/-}$;Rv$^{-/}$; Gcaps$^{-/-}$cones	34	23 ± 1.4	550 ± 51	67 ± 2.4	94 ± 8.5	2.2 ± 0.1	660 ± 27	6.8 ± 0.2
				42 ± 2.3	110 ± 7.3			

For parameters that are dependent on light intensity, two values are reported corresponding to ~25% (top) and 90% (bottom) of r_{max}. Values are means ± SEM. Statistical comparisons are given in the text.

variable from cell to cell, depending upon the position of the recorded cell in the slice and the amount of overlying debris. This variability contributes to the variability in our measurements of the parameters of the cells in Tables 1 and 2, particularly in our estimations of response sensitivity, which are unlikely to be more accurate than within a factor of two from one cell to the next.

Imaging

Individual cones were imaged after the completion of all experimental stimulation protocols (see Fig. 1, C and D). A fluorescent dye (100 µm; Alexa Fluor 750, λ_{max} ~750 nm; ThermoFisher) was included in the internal pipette solution and diffused into the target cell during recording. To collect images, we used a Nikon eclipse E600FN microscope with a Fluor 60×/1.00 water-immersion DIC objective (without DIC), at a temperature of 34–36°C with normal bath perfusion. Images were collected with a Rolera-Xr camera (FAST1394; Q imaging) and acquired and processed with Nikon Elements software (Nikon). Two types of images were collected. Infrared light was used to capture a wide-field image of the recording site without bleaching significant amounts of visual pigment. Bright red light (X-cite series 120; Excelitas Technologies) was filtered through a Cy7 cube (Nikon) and stimulated the Alexa dye to reveal the single, recorded cone. Fluorescent images were pseudocolored in Adobe Photoshop CS6 and merged with the wide-field images to demonstrate location and morphology of the recorded cell.

Data analysis

Data traces were analyzed and statistical significance evaluated in MATLAB with custom scripts or packaged routines. Data were filtered digitally at 50 Hz unless otherwise indicated. Data were typically baseline subtracted by linear subtraction. To make a rapid assessment of spectral sensitivity and opsin content, the peak amplitude of the response to a dim intensity (typically <0.3 of r_{max}, the maximum photocurrent to a saturating intensity) was divided by the number of pigment molecules bleached by the flash (P*). To derive sensitivities from response families, normalized photoresponses were plotted against the number of pigment molecules bleached, and data were fit with the Michaelis–Menten equation:

$$\frac{r}{r_{max}} = \frac{I}{(I + I_{1/2})}, \tag{1}$$

where r is the response at a given intensity, r_{max} is the maximum photocurrent to a saturating intensity, I is the number of pigment molecules bleached by the flash (P*), and $I_{1/2}$ is the value of P* required to produce a half-maximal response. $I_{1/2}$ was then used as a measure of sensitivity (Tables 1 and 2).

To estimate amplification constants, we proceeded in the following way. The first one third to one half of the rising phase of each flash response before digital filtering was fit with

$$r = r_{max}\left(1 - e^{\left(-a\left(t-t_{eff}\right)^2\right)}\right), \tag{2}$$

where t_{eff} (s) is a time delay from stimulus onset to initiation of the photoresponse (Pugh and Lamb, 1993). To calculate the amplification constant (A) for a specific flash response, the derived parameter a was multiplied by 2 and divided by the number of pigment molecules (P*) activated by the flash.

Results

Although previous patch-clamp recordings of cone responses have been made by inserting electrodes into the

Ingram et al.
Voltage-clamp responses of mouse cones

Journal of General Physiology 1290
https://doi.org/10.1085/jgp.201912419

Table 2. Mouse cone steady-light response parameters

Genotype	n	$r_{max,pk}$ (pA)	$r_{max,ss}$ (pA)	$I_{1/2,ss}$ (P*/s)	Time to peak (ms)	τ_{rec1} (ms)	τ_{rec2} (s)	A1/A2	Recovery (%)
$Gnat1^{-/-}$ cones	9	21 ± 3.2	18 ± 2.5	250,000 ± 95,000	140 ± 17	105 ± 8	1.4 ± 0.34	1.5 ± 0.66	51 ± 3
$Gnat1^{-/-};Rv^{-/-}$ cones	11	20 ± 1.5	17 ± 1.5	600,000 ± 175,000	110 ± 11	223 ± 64	1.3 ± 0.26	1.7 ± 0.70	41 ± 4
$Gnat1^{-/-};Gcaps^{-/-}$ cones	10	19 ± 2.3	16 ± 1.8	68,000 ± 13,000	155 ± 15	330 ± 38			19 ± 3
$Gnat1^{-/-};Rv^{-/-};$ $Gcaps^{-/-}$cones	9	24 ± 2.6	20 ± 2.7	63,000 ± 27,000	180 ± 11	490 ± 76			18 ± 4

Values are means ± SEM. Statistical comparisons are given in the text. $I_{1/2,ss}$, sensitivity of steady-state current response; $r_{max,pk}$, peak current response, measured <200 ms after stimulus onset; $r_{max,ss}$, steady-state current response, averaged from the last 1 s of the brightest stimulus.

retina blindly (Cangiano et al., 2012; Asteriti et al., 2014, 2017), we thought it might be useful to develop a method to record from the photoreceptors under visual control. Although we contemplated recording from retinas with cones or cone sheaths labeled with a fluorescent dye, we were concerned that the light used to excite the dye might light-adapt the retina. We therefore developed a method of identifying individual mouse cone somata by distinguishable visual cues alone (see Materials and methods). Cell type was further confirmed through electronic signatures, sensitivity to light, and morphology by dye filling. Sensitivity and membrane capacitance (C_m) were measured before other experimental protocols were initiated. C_m was generally at least twofold higher in mouse cones than in rods. For all 168 cones in Table 1, C_m averaged 7 ± 1 pF, and for five representative rods, C_m was 3 ± 1 pF (p < 0.0003, Student's

Figure 1. **Photoresponses of mouse cones recorded with whole-cell patch clamp. (A)** Current responses recorded from a WT mouse cone with minimal rod input. The soma of the cone was voltage clamped and held at −50 mV. Brief flashes of increasing strength (22–2,100 P*/flash) were presented at time = 0 ms. **(B)** Voltage responses from the same cone as A, stimulated with the same light flashes. Data traces in A and B are averages of seven presentations for each of the flashes and were filtered digitally during analysis (50 Hz). **(C)** An individual cone visualized with a far-red dye (Alexa Fluor 750) perfused into the cell from the recording pipette. **(D)** Merged image of C (pseudocolored red) and wide-field image of the same retinal slice. Scale bar, 20 μm.

t test). This difference is in consonance with the larger plasma-membrane area of the cone outer segment (Young, 1969). The difference in C_m produced highly distinct waveforms in response to small voltage pulses, and photoreceptor type could be easily determined.

Rod and cone sensitivities were initially estimated with a single flash given in the mesopic range (100–200 P*/flash). At this flash value, rods produced saturating or near-saturating photoresponses, while only ∼20% of the cone dark current was suppressed. By measuring C_m and mesopic flash sensitivity, we could identify photoreceptor type quickly and accurately. This identification was confirmed by filling selected cells with a far-red fluorescent dye (Alexa Fluor 750), loaded from the recording pipette and visualized at the completion of the experiment. Cone somata were localized to the outermost part of the ONL (see Fig. 1, C and D). The cone outer segments were shorter than those of rods, their somata were larger, and their pedicles extended to the inner portion of the outer plexiform layer (Fig. 1 D).

Once identified, cones were stimulated with brief flashes of light of increasing brightness. Cones that remained stable were then stimulated with a variety of other light protocols until significant bleaching and/or rundown became apparent. In many cases, we were able to record dark-adapted photoresponses in both voltage clamp (Fig. 1 A) and current clamp (Fig. 1 B) from the same cone. In voltage-clamp mode, the maximum amplitude of the light response was 20–25 pA at −50 mV. This value is similar to rod dark currents routinely recorded in our laboratory either from slices under similar conditions or from suction-electrode recording (see, for example, Ingram et al., 2016). In current-clamp mode, resting membrane potentials were typically between −45 and −55 mV (see Materials and methods).
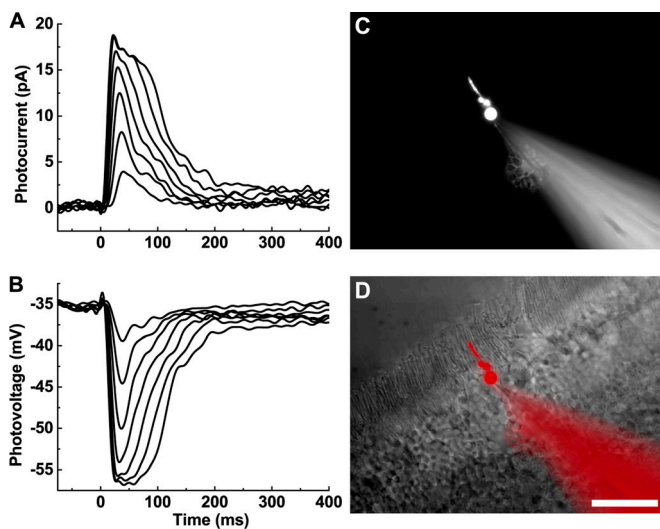
Characteristics of WT cone responses
Some WT cone current responses displayed monophasic or nearly monophasic waveforms with rapid recovery kinetics (Fig. 1 A). In most cones, however, this faster waveform was followed by a component of slower decay that varied in amplitude, typically ∼5 pA but as large as 15 pA. This slower component was likely to be produced by rod input entering the cone through gap junctions (Raviola and Gilula, 1975; Schneeweis and Schnapf, 1995, 1999; Hornstein et al., 2005; Asteriti et al., 2014, 2017). Fig. 2 A illustrates the waveform
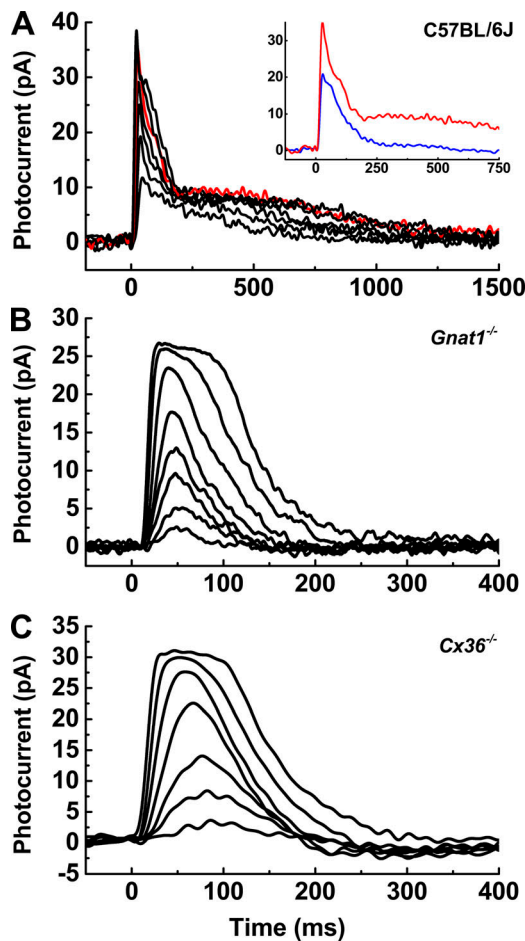
Figure 2. **Rods contribute to WT cone photocurrents.** Superimposed photocurrents from individual cones with stimuli ranging from 40 to 6,000 P*/flash. **(A)** WT cone with strong rod coupling. Red trace represents the dark-adapted response to a flash bleaching 1,520 P*. Inset: Red trace from A compared with blue trace, giving photoresponse to same flash but in the presence of a background light bleaching 9,300 Rh* s^{-1} (or 3,400 M-opsin pigment molecules bleached s^{-1} in the smaller cones). **(B)** Recovery of photocurrent in Gnat1$^{-/-}$ cone is monophasic, lacking the slower secondary component seen in A. **(C)** Similar result for Cx36$^{-/-}$ cone. Note that time base is faster in B and C than in A.

observed in a cone with particularly strong rod input. With adequate recovery time between flashes, the slower rod component was stable and did not increase as was previously reported (Asteriti et al., 2014).

It was possible to suppress the slow component with dim/mesopic background light. The inset to Fig. 2 A compares a dark-adapted response from this cell (red trace) to a response to the same flash in the presence of a background (blue trace) bleaching 9,300 rod pigment molecules per second (Rh* s^{-1}). Several additional lines of evidence indicated that electrical spread from rods was the source of the slower recovery phase. The time course of the slow component increased with the brightness of the flash (Fig. 2 A) and was comparable to the time course of rods stimulated with flashes bleaching similar amounts of rod pigment. The slow component was never observed if the generation or transmission of the rod photoresponse

was interrupted by genetic mutation. In Gnat1$^{-/-}$ retinas, rod-specific transducin α is knocked out, yielding electrically silent but otherwise healthy rods (Calvert et al., 2000). Cx36$^{-/-}$ cones lack the gap-junction protein that forms electrical synapses with neighboring rods (Deans et al., 2002; Asteriti et al., 2017). Cones from Gnat1$^{-/-}$ and Cx36$^{-/-}$ retinas recovered rapidly from brief flashes with consistently monophasic waveforms (Fig. 2, B and C). In subsequent experiments, we therefore used Gnat1$^{-/-}$ and Cx36$^{-/-}$ transgenic lines with the goal of measuring isolated cone responses without interference from rod signals.

Physiological characteristics of light responses of WT and mutant cones

We measured the photocurrents of all the genetic lines by presenting a series of 5-ms flashes of increasing strength. Normalized peak-current responses were plotted against the number of bleached pigment molecules (Fig. 3 A) and were fit with Eq. 1 (see Materials and methods). These fits gave the value of P* required to produce a half-maximal response ($I_{1/2}$; Table 1). The values of $I_{1/2}$ in P* per flash were similar in Gnat1$^{-/-}$ and Cx36$^{-/-}$ cones (940 ± 110, red data and fit; 990 ± 93, blue data and fit; p > 0.99, one-way ANOVA). The total (rod plus cone) response to flashes from WT cones saturated at intensities similar to the values for Gnat1$^{-/-}$ and Cx36$^{-/-}$ cones (p = 0.75), but WT cones responded more robustly to dimmer flashes (pink data points). Sensitivity measured with dim flashes was significantly greater for WT than for both Gnat1$^{-/-}$ and Cx36$^{-/-}$ cones (p = 0.002 and 0.025). Flash sensitivity was measured in several rods for comparison ($I_{1/2}$ = 14 ± 2 Rh*, black data and fit).

The amplification constant A is a quantification of the rate at which P* activates the transduction cascade (Cobbs and Pugh, 1987; Pugh and Lamb, 1993). Values of A were derived for Cx36$^{-/-}$ cones across the full dynamic range (Fig. 3 B) and were ~1 s^{-1}. The smaller value at the brightest intensity was not significantly different from the values at the other intensities. Somewhat larger values were obtained for WT and Gnat1$^{-/-}$ cones (Table 1), consistent with previous estimates for WT and Gnat1$^{-/-}$ cones from suction-electrode recording (Nikonov et al., 2006). It is unclear why the rate of transduction should differ for Cx36$^{-/-}$ and Gnat1$^{-/-}$ cones; the difference was however highly significant (p < 0.0005) and could in some way reflect the better space clamp of the Cx36$^{-/-}$ cones in the absence of electrotonic spread of current through gap junctions. The value of A for rods was at least twofold larger and was significantly different from A for the 168 cones of Table 1 (p = 0.0027, two-way ANOVA). In Table 1, we also give exponential time constants of flash-response recovery (τ_{rec}) and time-to-peak amplitude.

Dependence of response properties on pigment content

Mouse retina has two cone pigments with peak absorption at ~355 nm (S type) and 508 nm (M type, Lyubarsky and Pugh, 1996; Nikonov et al., 2006) and three kinds of cones: S, M, and dual cones having both S and M pigments. Dual cones generally have much more S than M pigment (Röhlich et al., 1994; Applebury et al., 2000; Haverkamp et al., 2005; Nikonov et al., 2006; Ortín-Martínez et al., 2014). We assessed the dependence
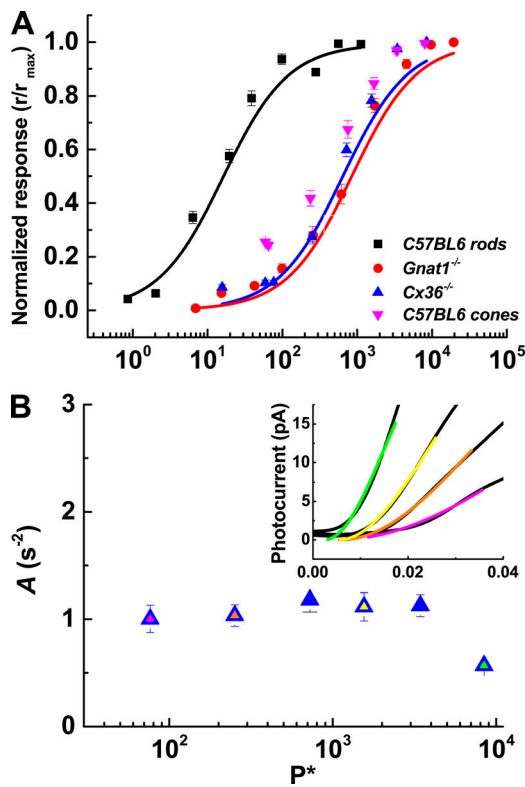
Figure 3. **Intensity–response relationships and amplification constants.** **(A)** Normalized photocurrent response (r/r_{max}) plotted against the number of cone pigment molecules bleached (P*) by the flash (P*/flash). Lines are best fits to Eq. 1 with k set to unity. Values of $I_{1/2}$ were as follows: WT, 14 ± 2, $n = 5$; $Gnat1^{-/-}$ cones, 940 ± 110, $n = 25$; $Cx36^{-/-}$ cones, 990 ± 93, $n = 30$. **(B)** Eq. 2 was fit to the first one third to one half of the rising phase of each flash response (inset) to derive amplification constants (A; s^{-2}). Values of A from $Cx36^{-/-}$ cones were plotted against flash strength. Inset: Fits to several flashes from the cone in Fig 2 C. The colors of fit lines match the filled symbols.
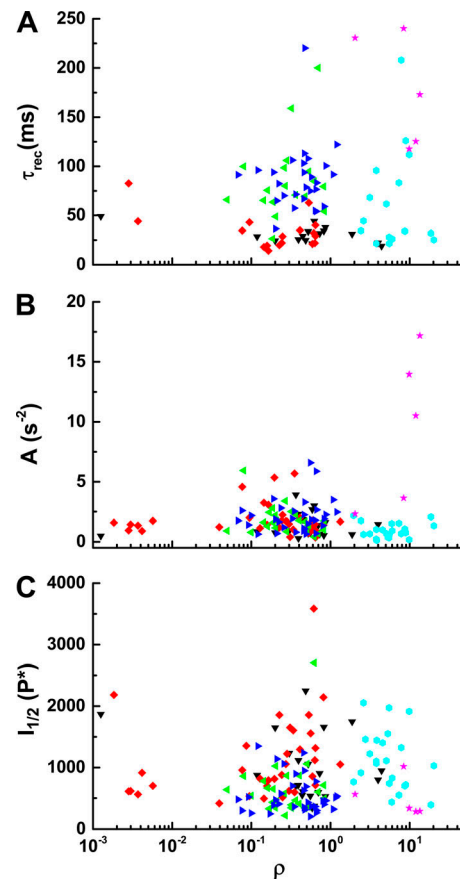

Figure 4. **Dependence of cone response properties on pigment content.** Physiological properties of cones were measured from different mouse lines and plotted versus M-opsin coexpression ratios (ρ, see text) from a total of 142 cones. τ_{rec} (A), amplification constants A (B), and $I_{1/2}$ (C). Genotypes: $Gnat1^{-/-}$, black; $Gnat1^{-/-};Rv^{-/-}$, red; $Gnat1^{-/-};Gcaps^{-/-}$, green; $Gnat1^{-/-};Rv^{-/-}; Gcaps^{-/-}$, blue; $Cx36^{-/-}$, cyan; and C57BL/6J (WT), pink.

of pigment content on cone properties by giving test flashes with 365-nm and 505-nm LEDs. For each cone, we produced an M-opsin coexpression ratio (ρ) by dividing the flash sensitivity at 505 nm by the 365-nm sensitivity (Nikonov et al., 2006). Because many, if not most, mouse cones express both types of pigment (Applebury et al., 2000), and the β-bands of M-pigments are sensitive to short and UV wavelengths (Govardovskii et al., 2000), ρ measurements across a large population of cones formed a continuum rather than two distinct groupings. The response parameters $I_{1/2}$, τ_{rec}, and A are compared with ρ values in Fig. 4 and did not reveal any obvious correlations. WT cones had a higher sensitivity to 505 nm, likely due to rod input for dim flashes. It is unclear why the value of ρ was consistently larger for $Cx36^{-/-}$ cones and smaller for $Gnat1^{-/-};Rv^{-/-}$ cones. We made no attempt to control the part of the retina from which recordings were made and may have oversampled dorsal retina in one case and ventral retina in the other, where M or S pigment expression are known to be dominant (Applebury et al., 2000; Ortín-Martínez et al., 2014). It is also possible that strain differences may have contributed to the ratios we observed.

Role of calcium-sensitive transduction proteins in shaping the cone photocurrent

Mice with genetic knockouts for recoverin and/or GCAPs were bred onto the $Gnat1^{-/-}$ background yielding lines that were double knockout ($Gnat1^{-/-};Rv^{-/-}$ and $Gnat1^{-/-};Gcaps^{-/-}$) and triple knockout ($Gnat1^{-/-};Rv^{-/-};Gcaps^{-/-}$). Cones with these genetic backgrounds were stimulated with brief flashes and 5-s steps of steady light. Representative examples are given in Fig. 5, with the flash responses (left column) and step responses (right column) from the same cone. Alterations in the waveform of the flash response for $Gnat1^{-/-};Rv^{-/-}$ and $Gnat1^{-/-};Gcaps^{-/-}$ cones were qualitatively similar to those reported earlier for $Rv^{-/-}$ and $Gcaps^{-/-}$ rods (Mendez et al., 2001; Makino et al., 2004), as well as for $Gnat1^{-/-};Rv^{-/-}$ and $Gnat1^{-/-};Gcaps^{-/-}$ cones recorded with suction electrodes and whole-retina recording (Sakurai et al., 2011, 2015). The loss of GCAPs caused cones to recover more slowly for any given flash of light (Fig. 5 A versus Fig. 5, E and G). Concomitantly, the longer response increased the integration time, which increased flash sensitivity (Fig. 6 A and Table 1). Flash responses of $Gnat1^{-/-};Rv^{-/-}$ and $Gnat1^{-/-}$ cones were remarkably similar. The τ_{rec} and time to peak of the photocurrent in $Gnat1^{-/-};Rv^{-/-}$ cones were slightly faster than $Gnat1^{-/-}$ cones,
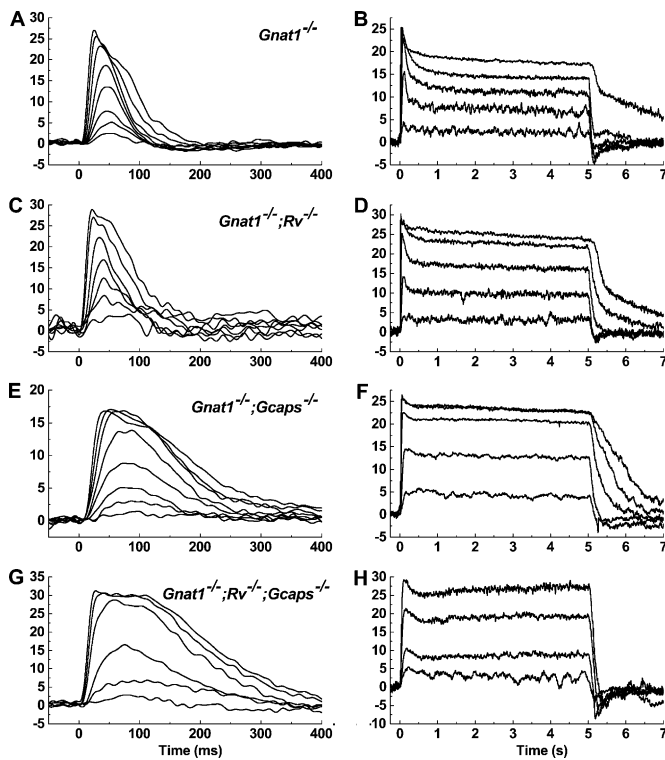
Figure 5. **Flash and step responses from WT cones and cones lacking recoverin and/or the GCAPs.** Photocurrents were recorded from transgenic mouse cones: $Gnat1^{-/-}$ (A and B), $Gnat1^{-/-};Rv^{-/-}$ (C and D), $Gnat1^{-/-};Gcaps^{-/-}$ (E and F), and $Gnat1^{-/-};Rv^{-/-};Gcaps^{-/-}$ (G and H). Stimulus onset was at time = 0 ms. The left column shows current responses from individual, representative cones when exposed to brief flashes of increasing strength (in P*/flash): $Gnat1^{-/-}$ 63–15,000; $Gnat1^{-/-};Rv^{-/-}$ 190–39,000; $Gnat1^{-/-};Gcaps^{-/-}$ 76–9,400; $Gnat1^{-/-};Rv^{-/-};$ $Gcaps^{-/-}$ 81–7,770. Traces are averages of three to five traces/flash strength. In the right column, the same cones were stimulated with 5 s of steady light at increasing intensities (in P*/s): $Gnat1^{-/-}$ 3,400–1.5 × 10^6; $Gnat1^{-/-};Rv^{-/-}$ 3,700–4.0 × 10^6; $Gnat1^{-/-};Gcaps^{-/-}$ 4,900–1.03 × 10^6; $Gnat1^{-/-};$ $Rv^{-/-};Gcaps^{-/-}$ 7,500–64,000. Each steady-light intensity was presented two times to limit pigment bleaching.

but the differences were not significant (n = 36 and 25, two-way ANOVA, p = 0.65 and p = 0.996). This is in contrast to the loss of recoverin in rods, which produces measurably faster flash responses (Makino et al., 2004; Chen et al., 2010a, 2012, 2015; Morshedian et al., 2018). Additionally, $I_{1/2}$ was somewhat higher in $Gnat1^{-/-};Rv^{-/-}$ cones and lower in $Gnat1^{-/-};Gcaps^{-/-}$ cones (Table 1), though these differences were again not significant (p = 0.95 and p = 0.12), perhaps in part the result of variability in cone collecting area (see Materials and methods).

The right column of Fig. 5 shows representative waveforms of cones of these same genotypes to 5-s steps of light. Responses of $Gnat1^{-/-}$ cones reached an initial peak and then declined (Fig. 5 B). Since light causes a decrease in the free-calcium concentration of the outer segments of both rods and cones (Sampath et al., 1999; Woodruff et al., 2002), which has been shown to have an important role in cone adaptation (Nakatani and Yau, 1988; Matthews et al., 1990), we examined the contribution of the small-molecular-weight Ca-binding proteins recoverin and the GCAPs in shaping the step response. Curves of normalized steady-state response as a function of step intensity for all of the
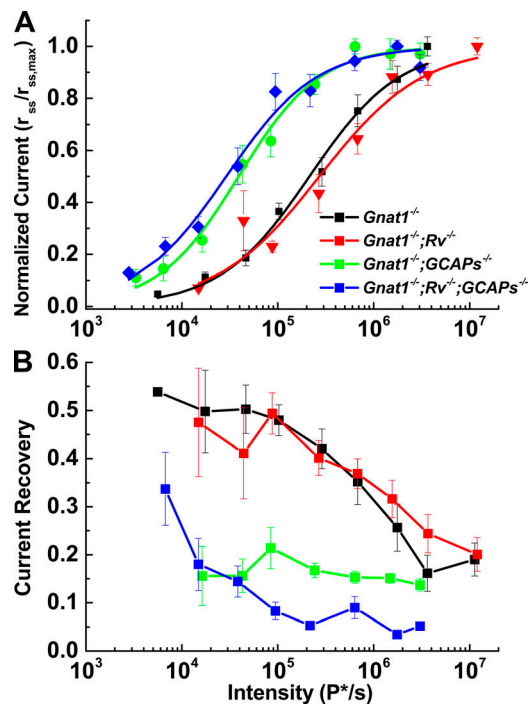

Figure 6. **Kinetics and sensitivity changes occur when transduction proteins are lost. (A)** Intensity–response relations for the steady-state current response normalized to the peak steady-state current response are plotted against stimulus intensity and fit with Eq. 1. **(B)** The percentage of current recovery (i.e., percentage of channels reopening) was calculated as the difference between the peak and steady-state currents divided by the peak current. $Gnat1^{-/-}$ and $Gnat1^{-/-};Rv^{-/-}$ cones quickly recovered a large fraction of their initial dark current (30–50%) before reaching steady-state. $Gcaps^{-/-}$ cones recovered much less dark current (~20%) Error bars represent SEM.

various mouse lines are given in Fig. 6 A. Values of $I_{1/2}$ are given in Table 2. These values were significantly different between the $Gnat1^{-/-};Rv^{-/-}$ cones and either the $Gnat1^{-/-};Gcaps^{-/-}$ cones or the $Gnat1^{-/-};Rv^{-/-};Gcaps^{-/-}$ cones (p = 0.011 and 0.013). They were not significantly different between $Gnat1^{-/-}$ cones and either of the lines lacking the GCAPs, perhaps again as a result of variability in cone collecting area.

Response recovery as a function of light intensity was quantified by calculating the time constant of photocurrent decay (Table 2) and fractional photocurrent recovery from the initial peak response to the steady-state photocurrent value (Fig. 6 B and Table 2). $Gnat1^{-/-};Rv^{-/-}$ cones retained a capacity to recover similar to $Gnat1^{-/-}$ cones (n = 11 and 9, two-way ANOVA, p = 0.723), and cones of both genotypes rapidly reopened a significant fraction of the cGMP-gated channels. In contrast, cones with deletion of the GCAPs recovered much less of their dark current (two-way ANOVA, p < 0.005). It is striking, however, that even these cones still showed significant relaxation in the response to bright light and appeared not to saturate (see also Fig. 7 B and Sakurai et al., 2011).

To quantify the rate of decay and approach to steady state for the responses to the various mouse lines, we noted first that the responses of $Gnat1^{-/-}$ and $Gnat1^{-/-};Rv^{-/-}$ cones were poorly fit with single-exponential functions but much better described by a double exponential,
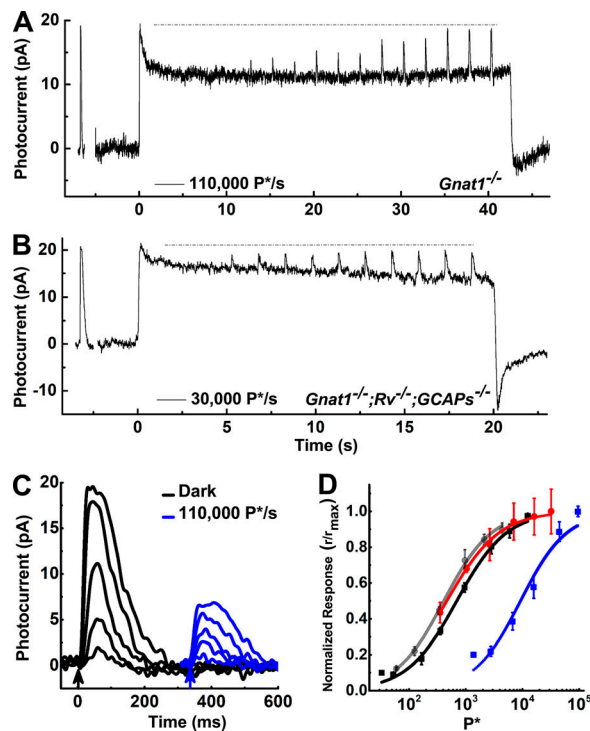
Figure 7. **Cones escape saturation and reopen CNG channels in bright light.** Current responses from a *Gnat1⁻/⁻* cone (A) and a *Gnat1⁻/⁻;Rv⁻/⁻; Gcaps⁻/⁻* cone (B) to a brief, saturating flash (~5,000 P*/flash) followed by exposure to steady light. The trace in A is a single exposure of >40 s at 110,000 P*/s. The trace in B gives average photocurrent responses from two exposures of 405-nm light bleaching 30,000 ± 7,000 P*/s for 20 s. 5 s after the steady light was turned on, flashes of increasing strength were delivered to the cone (1,800 ± 100 to 29,000 ± 1,000 P*/flash). The dashed line illustrates the initial peak–current response. **(C)** Average photocurrent responses to brief flashes (arrows) were measured in the *Gnat1⁻/⁻* cone from A during dark conditions (black traces) and during a steady background (blue traces). **(D)** Similar backgrounds were presented to *Gnat1⁻/⁻* cones (n = 5) and *Gnat1⁻/⁻; Rv⁻/⁻;Gcaps⁻/⁻* cones (n = 5). The peak current responses of the flashes were normalized to the maximal response in the presence of the background and plotted against the number of pigment molecules bleached by the flashes (P*). Data were fit with Eq. 1 to obtain values of $I_{1/2}$. The sensitivity of *Gnat1⁻/⁻* cones was determined to be 700 ± 13 P* in the dark (black) and 9,400 ± 1,500 P* during steady illumination (blue). The sensitivity of *Gnat1⁻/⁻; Rv⁻/⁻;Gcaps⁻/⁻* cones was 410 ± 16 P* in the dark (gray) and 470 ± 13 P* during steady illumination (red). The principal effect of background light on the triple knockouts was to decrease the number of open channels. Error bars represent SEM.

$$\frac{r}{r_{max}} = A_1 e^{t/\tau 1} + A_2 e^{t/\tau 2}. \quad (3)$$

The *Gnat1⁻/⁻;Gcaps⁻/⁻* cones and triple mutants were, on the other hand, adequately described by a single exponential. In Table 2, we give the best fitting values of the time-to-peak and exponential decay time constants for responses having a normalized steady-state photocurrent near 0.5 r_{max}. We show the two tau values as well as the ratio of A_1 to A_2 for the *Gnat1⁻/⁻* and *Gnat1⁻/⁻;Rv⁻/⁻* cones and only a single time constant for the *Gnat1⁻/⁻;Gcaps⁻/⁻* cones and triple mutants. Because even for the *Gnat1⁻/⁻* and *Gnat1⁻/⁻;Rv⁻/⁻* cones the shorter of the two time constants was dominant, we did statistical comparisons only of

these time constants across all of the mutant lines. Both the *Gnat1⁻/⁻* and *Gnat1⁻/⁻;Rv⁻/⁻* cones recovered more rapidly than either the *Gnat1⁻/⁻;Gcaps⁻/⁻* cones or triple mutants (p between 1.10^{-4} and 1.2×10^{-6}), but there were no significant differences between the *Gnat1⁻/⁻* and *Gnat1⁻/⁻;Rv⁻/⁻* cones on the one hand or between *Gnat1⁻/⁻;Gcaps⁻/⁻* cones and triple knockouts on the other (p for both = 0.99).

Adaptation during prolonged illumination

The relaxation following the onset of steady light seen in all of the photoresponses in the right column of Fig. 5 and in Fig. 6 B could represent the reopening of cyclic nucleotide–gated (CNG) channels, or it could arise from a conductance residing in the inner segment. Because voltage-clamp recordings more accurately monitor the cone outer-segment conductance than previous measurements of whole-retina electroretinograms (Sakurai et al., 2011), we examined whether CNG channels were reopening by exposing cones to bright, steady light and then allowing the response to come to steady state before additional bright flashes were presented on top of the background (Fig. 7). With sufficiently bright flashes, it was possible to further suppress the photocurrent from steady state to a value close to the initial peak response. Responses to these bright incremental flashes superimposed on the background light never exceeded the initial response to the onset of the background, indicated by the dashed lines in the figure. This observation supports the view that bright light causes a temporarily closure of all the CNG channels in cones which then reopen during adaptation to the background.

Gnat1⁻/⁻ cones exposed to a background intensity of 110,000 P*/s produced a 13-fold decrease in sensitivity (Fig. 7 D, black and blue symbols and curves) while suppressing <60% of the circulating current at steady state (Figs. 6 B and 7 A). This is in stark contrast to rods, which remain nearly saturated at much lower intensities (Chen et al., 2010b; Morshedian et al., 2018). Triple mutant cones retained the ability to adapt and reopen CNG channels over time (Fig. 7 B), though to a much less extent than *Gnat1⁻/⁻* (Fig. 7 A) and *Gnat1⁻/⁻;Rv⁻/⁻* cones (Fig. 4 D). This behavior contrasts with that recently reported for rods, where deletion of recoverin with or without deletion of the GCAPs suppresses photocurrent recovery during prolonged light exposure (Morshedian et al., 2018).

The desensitization produced by background light was also much less in the triple-knockout cones (Fig. 7 D, gray and red symbols and curves) than in *Gnat1⁻/⁻* cones. This observation is in agreement with previous work, indicating that the principal effect of background light on rods and cones lacking the GCAP molecules is to decrease the number of channels available to be closed (Mendez et al., 2001; Chen et al., 2010b; Sakurai et al., 2011).

Discussion

We describe a methodology for voltage clamping dark-adapted normal and mutant mouse cones without the use of fluorescent dyes or any other marking method. We have used this technique to characterize the physiological characteristics of the cones, including the sensitivity and kinetics of responses to flashes and

Ingram et al.
Voltage-clamp responses of mouse cones

Journal of General Physiology 1295
https://doi.org/10.1085/jgp.201912419

steps of light. We show that mouse cones recover from saturation even in the absence of the Ca²⁺-sensitive protein recoverin and the GCAPs, indicating that other still-unknown mechanisms must modulate cone photoresponse decay. Although previous measurements have been made from mouse cones with other approaches (Nikonov et al., 2005, 2006; Sakurai et al., 2011, 2015; Asteriti et al., 2014; Morshedian et al., 2019), our method has the advantage of lower noise and greater frequency response, together with the possibility of controlling both the internal and external solutions. A further advantage of patch-clamp recordings is the ability to make direct measurements of changes in outer-segment currents, which reflect the contributions of changes in outer-segment conductance together with a small component of current from NCKX transport (Perry and McNaughton, 1991). Since the properties of NCKX transport are well known (see, for example, Cervetto et al., 1989), they can be incorporated together with the changes in cGMP-gated conductance into any future model of cone transduction. In a subsequent publication (Ingram et al., 2019), we will show how our method can be used to measure the ion selectivity of the cGMP-gated conductance and the kinetics and voltage dependence of inner-segment conductances. This information will be essential for understanding how the current responses of cone outer segments produce voltage signals at the photoreceptor synaptic terminal.

Gap junctions and the rod secondary pathway
We have confirmed previous observations showing that rod responses spread into cone photoreceptors (Asteriti et al., 2014, 2017), probably through synaptic-terminal gap junctions (Schneeweis and Schnapf, 1995, 1999). The intensity–response relation in Fig. 3 suggests that the electrical coupling to rods has several actions. This circuit not only forms the entry point of rod signals into the cone bipolar circuitry but also boosts the cone response to dim-mesopic stimuli. Rod coupling biases the cone toward the rod spectral λ_{max}, which may decrease the mouse's ability to distinguish spectral differences in mesopic light.

While photoreceptor gap junctions have been reported to be under circadian control (Ribelayga et al., 2008; Jin and Ribelayga, 2016; Wong et al., 2018), we did not detect any correlation between the time of day (or night) when recordings were made and the amplitude of this slower component (data not shown). This result may reflect our use of the WT strain C57BL/6J, which has been reported to underexpress the important circadian modulator melatonin (Tosini et al., 2008). Several experiments were also performed in the CBA/Ca mouse line (data not shown), which maintains robust circadian rhythms. Even in CBA/Ca mice, no significant correlation between the time of day and the amplitude of rod signal spread was observed. It is possible that the process of slicing the retina disturbs any intact rhythms (Ruan et al., 2006).

Adaptation and escape from saturation
While considerable effort has gone into understanding why rods are more sensitive than cones (Ingram et al., 2016), less work has focused on how cones manage to escape response saturation at bright light intensities. When cones are exposed to bright steady light, responses initially saturate but then rapidly recover to attain

a new steady state with increased circulating current (Figs. 5, 6, and 7). Recovery of the response is largely the result of reopening of CNG channels (Fig. 7, A and B). Moreover, recovery even for the $Gnat1^{-/-};Gcaps^{-/-}$ and triple-mutant cones has a time constant of the order of 400 ms and is 90% complete after only 1 s. Even at the brightest step intensities we used, a 1-s illumination would have bleached <1% of the cone photopigment, much too little to have altered the cone pigment concentration. The recovery is unlikely to be produced by decay of metaII, which is faster in cones than in rods but still considerably slower than the time course of current recovery during exposure to maintained illumination (Okada et al., 1994; Xu et al., 1997; Kuwayama et al., 2005; Burns et al., 2006; Shi et al., 2007; Fu et al., 2008; Sakurai et al., 2015). Decay of metaII may, however, be responsible for the slow recovery of current we observed *after* exposure to step illuminations, at intensities that may have been bright enough to bleach more cone pigment than could be rapidly extinguished by rhodopsin kinase and arrestin (see Fig. 5, B, D, and F; and Sakurai et al., 2015).

Current recovery must therefore be occurring as the result of some modulation of the phototransduction cascade. Channels could be reopening because the cGMP concentration is increasing. This could be occurring because the rate of the phosphodiesterase (PDE) is decreasing or because the rate of the cyclase is accelerating, or both. It is also possible that the current increases at least in part from some alteration in the sensitivity of the cGMP-gated channels to cGMP so that they begin to reopen even without a change in cGMP concentration.

In a WT mouse, much of current recovery in the cone is produced by activation of the cyclase by the GCAPs. This effect accounts for the greater recovery in cones that express the GCAPs than in cones that lack these proteins (Figs. 5, 6 B, and 7). The GCAPs bind Ca²⁺ in darkness, and in the light, a decrease in outer-segment Ca²⁺ causes Ca²⁺ bound to the GCAPs to fall off and be replaced by Mg²⁺ (see Dizhoor et al., 2010). This substitution accelerates the rate of guanylyl cyclase and increases the outer-segment cGMP concentration. GCAP-dependent recovery is likely to be more rapid in cones than in rods, because cones have been reported to have a higher concentration of GCAPs (Cowan et al., 1998; Zhang et al., 2003).

In the $Gnat1^{-/-};Gcaps^{-/-}$ and triple-mutant cones, modulation of the cyclase by the GCAPs cannot occur, and current recovery must be produced by some other mechanism (see also Sakurai et al., 2011). One possibility is that the rate of the PDE is regulated, for which there is some evidence in rods (Fain, 2011). In rods lacking the GCAPs, there is a slow recovery of the light response during a prolonged light step (Burns et al., 2002; Chen et al., 2010b; Morshedian et al., 2018). This recovery may be mediated by recoverin, because when both the GCAPs and recoverin genes are deleted, no recovery of the rod photocurrent occurs even during a 60-s saturating light step (Morshedian et al., 2018). Recoverin cannot have a similar effect in cones, because there is little difference between the time course and extent of recovery between the $Gnat1^{-/-};Gcaps^{-/-}$ and $Gnat1^{-/-};Rv^{-/-};Gcaps^{-/-}$ photoreceptors (Figs. 5, 6, and 7). It is of course possible that recoverin was washed out from $Gnat1^{-/-};Gcaps^{-/-}$ cones during our whole-cell recordings, but we think that the relatively high resistance of our patch pipettes makes this possible explanation unlikely.

The difference in recovery between rods and cones may be partially explained by a difference in the molecular composition of the PDE. We have previously shown (Majumder et al., 2015) that when cone PDE is expressed in a mouse rod, responses decay more rapidly. Rods expressing cone PDE have a higher basal rate of cGMP turnover and a faster rate of PDE inactivation than rods expressing rod PDE. This difference may account for the faster cone recovery even in the absence of the GCAPs. It is also possible that cone PDE is subject to some form of light-dependent or Ca^{2+}-activated modulation not present in the rods.

A final possibility is channel modulation. Rod cGMP-gated channels have been shown to be modulated by Ca^{2+}-calmodulin, which binds to the CNGβ1 subunit of the rod channel (Grunwald et al., 1998; Weitz et al., 1998) and can modulate the affinity of the channel for cGMP (Hsu and Molday, 1993; Gordon et al., 1995; Koutalos et al., 1995). However, deletion of the CNGβ1 channel–binding site for Ca^{2+}-calmodulin has no effect on the response of the rod to prolonged steps or on light adaptation (Chen et al., 2010b). The affinity of cone cGMP-gated channels has also been reported to be modulated by a process that is Ca^{2+} dependent but does not require calmodulin (Rebrik and Korenbrot, 1998, 2004), which uses a protein called CNG-modulin (Rebrik et al., 2012) or EML1 (Korenbrot et al., 2013). The role of this protein in mammalian cone response recovery and light adaptation is presently unknown.

Acknowledgments

References

Angueyra, J.M., and F. Rieke. 2013. Origin and effect of phototransduction noise in primate cone photoreceptors. *Nat. Neurosci.* 16:1692–1700. https://doi.org/10.1038/nn.3534

Applebury, M.L., M.P. Antoch, L.C. Baxter, L.L. Chun, J.D. Falk, F. Farhangfar, K. Kage, M.G. Krzystolik, L.A. Lyass, and J.T. Robbins. 2000. The murine cone photoreceptor: a single cone type expresses both S and M opsins with retinal spatial patterning. *Neuron.* 27:513–523. https://doi.org/10.1016/S0896-6273(00)00062-3

Asteriti, S., C. Gargini, and L. Cangiano. 2014. Mouse rods signal through gap junctions with cones. *eLife.* 3:e01386. https://doi.org/10.7554/eLife.01386

Asteriti, S., C. Gargini, and L. Cangiano. 2017. Connexin 36 expression is required for electrical coupling between mouse rods and cones. *Vis. Neurosci.* 34:E006. https://doi.org/10.1017/S0952523817000037

Baudin, J., J.M. Angueyra, R. Sinha, and F. Rieke. 2019. S-cone photoreceptors in the primate retina are functionally distinct from L and M cones. *eLife.* 8:e39166. https://doi.org/10.7554/eLife.39166

Baylor, D.A., and B.J. Nunn. 1986. Electrical properties of the light-sensitive conductance of rods of the salamander Ambystoma tigrinum. *J. Physiol.* 371:115–145. https://doi.org/10.1113/jphysiol.1986.sp015964

Burns, M.E., A. Mendez, J. Chen, and D.A. Baylor. 2002. Dynamics of cyclic GMP synthesis in retinal rods. *Neuron.* 36:81–91. https://doi.org/10.1016/S0896-6273(02)00911-X

Burns, M.E., A. Mendez, C.K. Chen, A. Almuete, N. Quillinan, M.I. Simon, D.A. Baylor, and J. Chen. 2006. Deactivation of phosphorylated and nonphosphorylated rhodopsin by arrestin splice variants. *J. Neurosci.* 26:1036–1044. https://doi.org/10.1523/JNEUROSCI.3301-05.2006

Calvert, P.D., N.V. Krasnoperova, A.L. Lyubarsky, T. Isayama, M. Nicoló, B. Kosaras, G. Wong, K.S. Gannon, R.F. Margolskee, R.L. Sidman, et al. 2000. Phototransduction in transgenic mice after targeted deletion of the rod transducin alpha -subunit. *Proc. Natl. Acad. Sci. USA.* 97:13913–13918. https://doi.org/10.1073/pnas.250478897

Cangiano, L., S. Asteriti, L. Cervetto, and C. Gargini. 2012. The photovoltage of rods and cones in the dark-adapted mouse retina. *J. Physiol.* 590:3841–3855. https://doi.org/10.1113/jphysiol.2011.226878

Cao, Y., H. Song, H. Okawa, A.P. Sampath, M. Sokolov, and K.A. Martemyanov. 2008. Targeting of RGS7/Gbeta5 to the dendritic tips of ON-bipolar cells is independent of its association with membrane anchor R7BP. *J. Neurosci.* 28:10443–10449. https://doi.org/10.1523/JNEUROSCI.3282-08.2008

Cervetto, L., L. Lagnado, R.J. Perry, D.W. Robinson, and P.A. McNaughton. 1989. Extrusion of calcium from rod outer segments is driven by both sodium and potassium gradients. *Nature.* 337:740–743. https://doi.org/10.1038/337740a0

Chang, B., N.L. Hawes, R.E. Hurd, M.T. Davisson, S. Nusinowitz, and J.R. Heckenlively. 2002. Retinal degeneration mutants in the mouse. *Vision Res.* 42:517–525. https://doi.org/10.1016/S0042-6989(01)00146-8

Chen, C.K., M.L. Woodruff, F.S. Chen, D. Chen, and G.L. Fain. 2010a. Background light produces a recoverin-dependent modulation of activated-rhodopsin lifetime in mouse rods. *J. Neurosci.* 30:1213–1220. https://doi.org/10.1523/JNEUROSCI.4353-09.2010

Chen, C.K., M.L. Woodruff, F.S. Chen, Y. Chen, M.C. Cilluffo, D. Tranchina, and G.L. Fain. 2012. Modulation of mouse rod response decay by rhodopsin kinase and recoverin. *J. Neurosci.* 32:15998–16006. https://doi.org/10.1523/JNEUROSCI.1639-12.2012

Chen, C.K., M.L. Woodruff, and G.L. Fain. 2015. Rhodopsin kinase and recoverin modulate phosphodiesterase during mouse photoreceptor light adaptation. *J. Gen. Physiol.* 145:213–224. https://doi.org/10.1085/jgp.201411273

Chen, J., M.L. Woodruff, T. Wang, F.A. Concepcion, D. Tranchina, and G.L. Fain. 2010b. Channel modulation and the mechanism of light adaptation in mouse rods. *J. Neurosci.* 30:16232–16240. https://doi.org/10.1523/JNEUROSCI.2868-10.2010

Cobbs, W.H., and E.N. Pugh Jr. 1987. Kinetics and components of the flash photocurrent of isolated retinal rods of the larval salamander, Ambystoma tigrinum. *J. Physiol.* 394:529–572. https://doi.org/10.1113/jphysiol.1987.sp016884

Cowan, C.W., R.N. Fariss, I. Sokal, K. Palczewski, and T.G. Wensel. 1998. High expression levels in cones of RGS9, the predominant GTPase accelerating protein of rods. *Proc. Natl. Acad. Sci. USA.* 95:5351–5356. https://doi.org/10.1073/pnas.95.9.5351

Deans, M.R., B. Volgyi, D.A. Goodenough, S.A. Bloomfield, and D.L. Paul. 2002. Connexin36 is essential for transmission of rod-mediated visual signals in the mammalian retina. *Neuron.* 36:703–712. https://doi.org/10.1016/S0896-6273(02)01046-2

Dizhoor, A.M., E.V. Olshevskaya, and I.V. Peshenko. 2010. Mg2+/Ca2+ cation binding cycle of guanylyl cyclase activating proteins (GCAPs): role in regulation of photoreceptor guanylyl cyclase. *Mol. Cell. Biochem.* 334:117–124. https://doi.org/10.1007/s11010-009-0328-6

Fain, G.L. 2011. Adaptation of mammalian photoreceptors to background light: putative role for direct modulation of phosphodiesterase. *Mol. Neurobiol.* 44:374–382. https://doi.org/10.1007/s12035-011-8205-1

Fu, Y., V. Kefalov, D.G. Luo, T. Xue, and K.W. Yau. 2008. Quantal noise from human red cone pigment. *Nat. Neurosci.* 11:565–571. https://doi.org/10.1038/nn.2110

Gordon, S.E., J. Downing-Park, and A.L. Zimmerman. 1995. Modulation of the cGMP-gated ion channel in frog rods by calmodulin and an endogenous

inhibitory factor. *J. Physiol.* 486:533–546. https://doi.org/10.1113/jphysiol.1995.sp020832

Govardovskii, V.I., N. Fyhrquist, T. Reuter, D.G. Kuzmin, and K. Donner. 2000. In search of the visual pigment template. *Vis. Neurosci.* 17: 509–528. https://doi.org/10.1017/S0952523800174036

Grunwald, M.E., W.P. Yu, H.H. Yu, and K.W. Yau. 1998. Identification of a domain on the beta-subunit of the rod cGMP-gated cation channel that mediates inhibition by calcium-calmodulin. *J. Biol. Chem.* 273:9148–9157. https://doi.org/10.1074/jbc.273.15.9148

Haverkamp, S., H. Wässle, J. Duebel, T. Kuner, G.J. Augustine, G. Feng, and T. Euler. 2005. The primordial, blue-cone color system of the mouse retina. *J. Neurosci.* 25:5438–5445. https://doi.org/10.1523/JNEUROSCI.1117-05.2005

Hornstein, E.P., J. Verweij, P.H. Li, and J.L. Schnapf. 2005. Gap-junctional coupling and absolute sensitivity of photoreceptors in macaque retina. *J. Neurosci.* 25:11201–11209. https://doi.org/10.1523/JNEUROSCI.3416-05.2005

Hsu, Y.T., and R.S. Molday. 1993. Modulation of the cGMP-gated channel of rod photoreceptor cells by calmodulin. *Nature.* 361:76–79. https://doi.org/10.1038/361076a0

Hughes, A.E., J.M. Enright, C.A. Myers, S.Q. Shen, and J.C. Corbo. 2017. Cell Type-Specific Epigenomic Analysis Reveals a Uniquely Closed Chromatin Architecture in Mouse Rod Photoreceptors. *Sci. Rep.* 7:43184. https://doi.org/10.1038/srep43184

Ingram, N.T., A.P. Sampath, and G.L. Fain. 2016. Why are rods more sensitive than cones? *J. Physiol.* 594:5415–5426. https://doi.org/10.1113/JP272556

Ingram, N., G. Fain, and A. Sampath. 2019. Voltage-clamp currents and light responses of mouse cones. *Invest. Ophthalmol. Vis. Sci.* 60:E-Abstract #1377.

Jin, N.G., and C.P. Ribelayga. 2016. Direct Evidence for Daily Plasticity of Electrical Coupling between Rod Photoreceptors in the Mammalian Retina. *J. Neurosci.* 36:178–184. https://doi.org/10.1523/JNEUROSCI.3301-15.2016

Korenbrot, J.I., M. Mehta, N. Tserentsoodol, J.H. Postlethwait, and T.I. Rebrik. 2013. EML1 (CNG-modulin) controls light sensitivity in darkness and under continuous illumination in zebrafish retinal cone photoreceptors. *J. Neurosci.* 33:17763–17776. https://doi.org/10.1523/JNEUROSCI.2659-13.2013

Koutalos, Y., K. Nakatani, and K.W. Yau. 1995. The cGMP-phosphodiesterase and its contribution to sensitivity regulation in retinal rods. *J. Gen. Physiol.* 106:891–921. https://doi.org/10.1085/jgp.106.5.891

Kuwayama, S., H. Imai, T. Morizumi, and Y. Shichida. 2005. Amino acid residues responsible for the meta-III decay rates in rod and cone visual pigments. *Biochemistry.* 44:2208–2215. https://doi.org/10.1021/bi047994g

Lyubarsky, A.L., and E.N. Pugh Jr. 1996. Recovery phase of the murine rod photoresponse reconstructed from electroretinographic recordings. *J. Neurosci.* 16:563–571. https://doi.org/10.1523/JNEUROSCI.16-02-00563.1996

Majumder, A., J. Pahlberg, H. Muradov, K.K. Boyd, A.P. Sampath, and N.O. Artemyev. 2015. Exchange of cone for rod phosphodiesterase 6 catalytic subunits in rod photoreceptors mimics in part features of light adaptation. *J. Neurosci.* 35:9225–9235. https://doi.org/10.1523/JNEUROSCI.3563-14.2015

Makino, C.L., R.L. Dodd, J. Chen, M.E. Burns, A. Roca, M.I. Simon, and D.A. Baylor. 2004. Recoverin regulates light-dependent phosphodiesterase activity in retinal rods. *J. Gen. Physiol.* 123:729–741. https://doi.org/10.1085/jgp.200308994

Matthews, H.R., G.L. Fain, R.L. Murphy, and T.D. Lamb. 1990. Light adaptation in cone photoreceptors of the salamander: a role for cytoplasmic calcium. *J. Physiol.* 420:447–469. https://doi.org/10.1113/jphysiol.1990.sp017922

Mendez, A., M.E. Burns, A. Roca, J. Lem, L.W. Wu, M.I. Simon, D.A. Baylor, and J. Chen. 2000. Rapid and reproducible deactivation of rhodopsin requires multiple phosphorylation sites. *Neuron.* 28:153–164. https://doi.org/10.1016/S0896-6273(00)00093-3

Mendez, A., M.E. Burns, I. Sokal, A.M. Dizhoor, W. Baehr, K. Palczewski, D.A. Baylor, and J. Chen. 2001. Role of guanylate cyclase-activating proteins (GCAPs) in setting the flash sensitivity of rod photoreceptors. *Proc. Natl. Acad. Sci. USA.* 98:9948–9953. https://doi.org/10.1073/pnas.171308998

Morshedian, A., M.L. Woodruff, and G.L. Fain. 2018. Role of recoverin in rod photoreceptor light adaptation. *J. Physiol.* 596:1513–1526. https://doi.org/10.1113/JP275779

Morshedian, A., J.J. Kaylor, S.Y. Ng, A. Tsan, R. Frederiksen, T. Xu, L. Yuan, A.P. Sampath, R.A. Radu, G.L. Fain, and G.H. Travis. 2019. Light-Driven Regeneration of Cone Visual Pigments through a Mechanism Involving RGR Opsin in Muller Glial Cells. *Neuron.* 102:1172–1183. e1175.

Nakatani, K., and K.W. Yau. 1988. Calcium and light adaptation in retinal rods and cones. *Nature.* 334:69–71. https://doi.org/10.1038/334069a0

Neher, E. 1992. Correction for liquid junction potentials in patch clamp experiments. *Methods Enzymol.* 207:123–131. https://doi.org/10.1016/0076-6879(92)07008-C

Nikonov, S.S., L.L. Daniele, X. Zhu, C.M. Craft, A. Swaroop, and E.N. Pugh Jr. 2005. Photoreceptors of Nrl -/- mice coexpress functional S- and M-cone opsins having distinct inactivation mechanisms. *J. Gen. Physiol.* 125:287–304. https://doi.org/10.1085/jgp.200409208

Nikonov, S.S., R. Kholodenko, J. Lem, and E.N. Pugh Jr. 2006. Physiological features of the S- and M-cone photoreceptors of wild-type mice from single-cell recordings. *J. Gen. Physiol.* 127:359–374. https://doi.org/10.1085/jgp.200609490

Okada, T., T. Matsuda, H. Kandori, Y. Fukada, T. Yoshizawa, and Y. Shichida. 1994. Circular dichroism of metaiodopsin II and its binding to transducin: a comparative study between meta II intermediates of iodopsin and rhodopsin. *Biochemistry.* 33:4940–4946. https://doi.org/10.1021/bi00182a024

Okawa, H., K.J. Miyagishima, A.C. Arman, J.B. Hurley, G.D. Field, and A.P. Sampath. 2010. Optimal processing of photoreceptor signals is required to maximize behavioural sensitivity. *J. Physiol.* 588:1947–1960. https://doi.org/10.1113/jphysiol.2010.188573

Ortín-Martínez, A., F.M. Nadal-Nicolás, M. Jiménez-López, J.J. Alburquerque-Béjar, L. Nieto-López, D. García-Ayuso, M.P. Villegas-Pérez, M. Vidal-Sanz, and M. Agudo-Barriuso. 2014. Number and distribution of mouse retinal cone photoreceptors: differences between an albino (Swiss) and a pigmented (C57/BL6) strain. *PLoS One.* 9:e102392. https://doi.org/10.1371/journal.pone.0102392

Perry, R.J., and P.A. McNaughton. 1991. Response properties of cones from the retina of the tiger salamander. *J. Physiol.* 433:561–587. https://doi.org/10.1113/jphysiol.1991.sp018444

Pugh, E.N. Jr., and T.D. Lamb. 1993. Amplification and kinetics of the activation steps in phototransduction. *Biochim. Biophys. Acta.* 1141:111–149. https://doi.org/10.1016/0005-2728(93)90038-H

Raviola, E., and N.B. Gilula. 1975. Intramembrane organization of specialized contacts in the outer plexiform layer of the retina. A freeze-fracture study in monkeys and rabbits. *J. Cell Biol.* 65:192–222. https://doi.org/10.1083/jcb.65.1.192

Rebrik, T.I., and J.I. Korenbrot. 1998. In intact cone photoreceptors, a Ca2+-dependent, diffusible factor modulates the cGMP-gated ion channels differently than in rods. *J. Gen. Physiol.* 112:537–548. https://doi.org/10.1085/jgp.112.5.537

Rebrik, T.I., and J.I. Korenbrot. 2004. In intact mammalian photoreceptors, Ca2+-dependent modulation of cGMP-gated ion channels is detectable in cones but not in rods. *J. Gen. Physiol.* 123:63–75. https://doi.org/10.1085/jgp.200308952

Rebrik, T.I., I. Botchkina, V.Y. Arshavsky, C.M. Craft, and J.I. Korenbrot. 2012. CNG-modulin: a novel Ca-dependent modulator of ligand sensitivity in cone photoreceptor cGMP-gated ion channels. *J. Neurosci.* 32:3142–3153. https://doi.org/10.1523/JNEUROSCI.5518-11.2012

Ribelayga, C., Y. Cao, and S.C. Mangel. 2008. The circadian clock in the retina controls rod-cone coupling. *Neuron.* 59:790–801. https://doi.org/10.1016/j.neuron.2008.07.017

Röhlich, P., T. van Veen, and A. Szél. 1994. Two different visual pigments in one retinal cone cell. *Neuron.* 13:1159–1166. https://doi.org/10.1016/0896-6273(94)90053-1

Ruan, G.X., D.Q. Zhang, T. Zhou, S. Yamazaki, and D.G. McMahon. 2006. Circadian organization of the mammalian retina. *Proc. Natl. Acad. Sci. USA.* 103:9703–9708. https://doi.org/10.1073/pnas.0601940103

Sakurai, K., J. Chen, and V.J. Kefalov. 2011. Role of guanylyl cyclase modulation in mouse cone phototransduction. *J. Neurosci.* 31:7991–8000. https://doi.org/10.1523/JNEUROSCI.6650-10.2011

Sakurai, K., J. Chen, S.C. Khani, and V.J. Kefalov. 2015. Regulation of mammalian cone phototransduction by recoverin and rhodopsin kinase. *J. Biol. Chem.* 290:9239–9250. https://doi.org/10.1074/jbc.M115.639591

Sampath, A.P., H.R. Matthews, M.C. Cornwall, J. Bandarchi, and G.L. Fain. 1999. Light-dependent changes in outer segment free-Ca²⁺ concentration in salamander cone photoreceptors. *J. Gen. Physiol.* 113:267–277. https://doi.org/10.1085/jgp.113.2.267

Schneeweis, D.M., and J.L. Schnapf. 1995. Photovoltage of rods and cones in the macaque retina. *Science.* 268:1053–1056. https://doi.org/10.1126/science.7754386

Schneeweis, D.M., and J.L. Schnapf. 1999. The photovoltage of macaque cone photoreceptors: adaptation, noise, and kinetics. *J. Neurosci.* 19: 1203–1216. https://doi.org/10.1523/JNEUROSCI.19-04-01203.1999

Shi, G., K.W. Yau, J. Chen, and V.J. Kefalov. 2007. Signaling properties of a short-wave cone visual pigment and its role in phototransduction. *J. Neurosci.* 27:10084–10093. https://doi.org/10.1523/JNEUROSCI.2211-07.2007

Sinha, R., M. Hoon, J. Baudin, H. Okawa, R.O.L. Wong, and F. Rieke. 2017. Cellular and Circuit Mechanisms Shaping the Perceptual Properties of the Primate Fovea. *Cell.* 168:413–426. e412.

Solovei, I., M. Kreysing, C. Lanctôt, S. Kösem, L. Peichl, T. Cremer, J. Guck, and B. Joffe. 2009. Nuclear architecture of rod photoreceptor cells adapts to vision in mammalian evolution. *Cell.* 137:356–368. https://doi.org/10.1016/j.cell.2009.01.052

Tosini, G., N. Pozdeyev, K. Sakamoto, and P.M. Iuvone. 2008. The circadian clock system in the mammalian retina. *BioEssays.* 30:624–633. https://doi.org/10.1002/bies.20777

Wang, J.S., and V.J. Kefalov. 2009. An alternative pathway mediates the mouse and human cone visual cycle. *Curr. Biol.* 19:1665–1669. https://doi.org/10.1016/j.cub.2009.07.054

Wang, J.S., M.E. Estevez, M.C. Cornwall, and V.J. Kefalov. 2009. Intra-retinal visual cycle required for rapid and complete cone dark adaptation. *Nat. Neurosci.* 12:295–302. https://doi.org/10.1038/nn.2258

Weitz, D., M. Zoche, F. Müller, M. Beyermann, H.G. Körschen, U.B. Kaupp, and K.W. Koch. 1998. Calmodulin controls the rod photoreceptor CNG channel through an unconventional binding site in the N-terminus of the beta-subunit. *EMBO J.* 17:2273–2284. https://doi.org/10.1093/emboj/17.8.2273

Wong, J.C.Y., N.J. Smyllie, G.T. Banks, C.A. Pothecary, A.R. Barnard, E.S. Maywood, A. Jagannath, S. Hughes, G.T.J. van der Horst, R.E. MacLaren, et al. 2018. Differential roles for cryptochromes in the mammalian retinal clock. *FASEB J.* 32:4302–4314. https://doi.org/10.1096/fj.201701165RR

Woodruff, M.L., A.P. Sampath, H.R. Matthews, N.V. Krasnoperova, J. Lem, and G.L. Fain. 2002. Measurement of cytoplasmic calcium concentration in the rods of wild-type and transducin knock-out mice. *J. Physiol.* 542:843–854. https://doi.org/10.1113/jphysiol.2001.013987

Xu, J., R.L. Dodd, C.L. Makino, M.I. Simon, D.A. Baylor, and J. Chen. 1997. Prolonged photoresponses in transgenic mouse rods lacking arrestin. *Nature.* 389:505–509. https://doi.org/10.1038/39068

Young, R.W. 1969. A difference between rods and cones in the renewal of outer segment protein. *Invest. Ophthalmol.* 8:222–231.

Zhang, X., T.G. Wensel, and T.W. Kraft. 2003. GTPase regulators and photoresponses in cones of the eastern chipmunk. *J. Neurosci.* 23:1287–1297. https://doi.org/10.1523/JNEUROSCI.23-04-01287.2003